

# Excimer Fluorescence as a Molecular Probe of Polymer Blend Miscibility. 7. Nonequilibrium Solvent Casting Effects in Blends of Poly(2-vinylnaphthalene) with Poly(*n*-butyl methacrylate) and Poly(methyl methacrylate)

Muhammad Amin Gashgari and Curtis W. Frank\*

Department of Chemical Engineering, Stanford University,  
Stanford, California 94305-5025. Received October 8, 1987

**ABSTRACT:** Blends of poly(2-vinylnaphthalene) (P2VN) with poly(*n*-butyl methacrylate) (PnBMA) or poly(methyl methacrylate) (PMMA) are prepared by solvent casting from toluene at temperatures from 295 to 353 K for P2VN concentrations from 0.10 to 10.0 wt %. Excimer fluorescence from P2VN is analyzed by a two-phase model for blend morphology. Deviations from thermodynamic equilibrium are interpreted in terms of kinetic restrictions arising during solvent evaporation from the ternary system. Annealing experiments in P2VN/PMMA blends yield a rate constant for increase in local P2VN concentration that increases as the blend becomes closer to its equilibrium-phase morphology.

## Introduction

This paper is part of a research program in which excimer fluorescence is employed to investigate miscible and immiscible polymer blends. The focus has been on relatively low concentration blends of the aromatic vinyl polymer poly(2-vinyl naphthalene) (P2VN) with various poly(alkyl methacrylates) and polystyrene.<sup>1-8</sup> In general, the majority of these blends are miscible only at very low P2VN concentration. A second series has focused on excimer fluorescence from polystyrene (PS) dispersed in poly(vinyl methyl ether) (PVME).<sup>9-13</sup> In this system blends may be prepared that are miscible over the entire composition range.

The present study is an extension of an earlier paper<sup>4</sup> in which the effect of solvent casting temperature was examined for blends of P2VN with poly(*n*-butyl methacrylate) (PnBMA) and poly(methyl methacrylate) (PMMA). Although photophysical data, in the form of the ratio of the excimer to monomer emission band intensities,  $I_D/I_M$ , were presented previously as a function of concentration and casting temperature, no detailed analysis of the fluorescence results was offered. Instead, the discussion emphasized the influence of the casting temperature,  $T_c$ , relative to the glass transition temperature,  $T_g$ , of the solvent-free binary polymer blend on equilibrium or nonequilibrium behavior. It was shown that experimentally observed cloud point curves for P2VN/PnBMA blends, which were solvent cast at  $T_c > T_g$ , could be satisfactorily fit with Flory-Huggins theory provided that proper account was taken of the temperature dependence of the solubility parameters used to calculate the binary interaction parameter. On the other hand, all P2VN/PMMA blends, which were cast at  $T_c < T_g$ , exhibited nonequilibrium behavior; i.e., apparent miscibilities for these blends were much higher than that predicted by the Flory-Huggins treatment.

The objective of the present paper is to provide a quantitative analysis of the equilibrium/nonequilibrium characteristics in the P2VN/PnBMA and P2VN/PMMA blends. Since the morphology resulting from the solvent casting process is quite dependent on the casting temperature, annealing experiments were performed to attempt to prepare films in their equilibrium states. Although the major interest is in the final fluorescence behavior after long periods of annealing at  $T > T_g$ , transient results are presented. A procedure is presented for correction of the new annealing data and the experimental results obtained previously<sup>4</sup> for the spectrofluorometer response. Finally, all such corrected data are analyzed in

terms of a photophysical model recently developed.<sup>10,14</sup>

## Experimental Section

All experimental details regarding the polymer samples, the casting process, and the spectrofluorometer have been presented previously.<sup>4</sup> The annealing experiments presented in this work were performed on samples cast from toluene at 295 K with different guest concentrations ranging between 0.10% and 10.0% by weight. Annealing was performed under nitrogen at 407 K. In order to record the spectra, an annealed sample was removed from the oven and cooled to room temperature. The spectrum was then taken and the sample returned to the oven.

## Results

**A. Annealing Measurements.** The observed excimer to monomer fluorescence ratio for the P2VN guest in the different concentration blends that were cast at 295 K is plotted as a function of annealing time at 407 K for the P2VN/PnBMA systems in Figure 1.  $I_D/I_M$  was determined by using measurements of the excimer at 398 nm and the monomer at 331 nm. No corrections for spectral overlap of the excimer and monomer have been made.  $I_D/I_M$  increased sharply during the first 24 h and remained constant thereafter up to 88 h of annealing time. Although the  $I_D/I_M$  value at the plateau increased as a function of bulk guest concentration, none of the films had a ratio approaching that for a neat P2VN film, which is 27.<sup>15</sup> Films with guest concentrations of 0.1% and 0.3% were optically clear before and after annealing, while those with guest concentrations of 1.0% and 3.0% changed from clear to cloudy during annealing. Films with guest concentrations of 5.0% and 10.0% were cloudy before the thermal treatment and remained cloudy thereafter.

Corresponding 407 K annealing data for the P2VN/PMMA blends cast at 295 K are shown in Figure 2.  $I_D/I_M$  for the PMMA host films also increased sharply during the first 24 h of annealing, but, in contrast to the PnBMA host films,  $I_D/I_M$  continued to increase beyond the 24 h, albeit at a reduced rate. Even after 145 h of annealing time, none of the films had reached the  $I_D/I_M$  value of a neat P2VN film, although the 10.0% film came close. Visual inspection of the PMMA host blends showed that all initially clear films (0.1% and 0.3%) remained clear and all initially cloudy films (1.0%, 3.0%, and 10.0%) continued to be cloudy after annealing. The observed ratios after 145 h of annealing time have been taken to be the final, constant  $I_D/I_M$  values for use in subsequent calculations.

**B. Data Reduction.** Two correction procedures had to be applied to the raw annealing data of Figures 1 and 2 as well as to the raw data for films cast at higher tem-

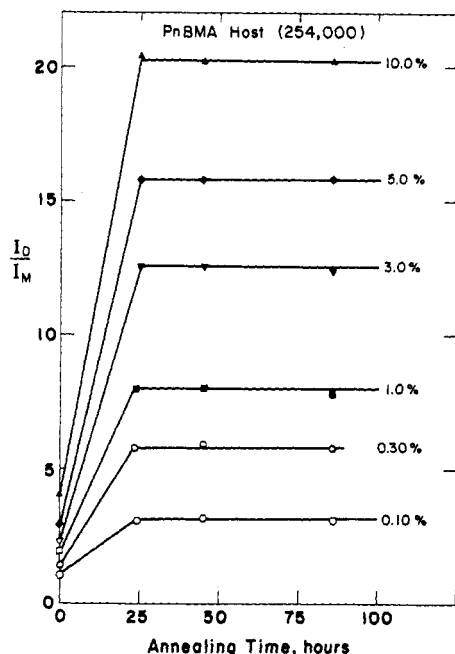


**Figure 1.** Observed  $I_D/I_M$  fluorescence ratio as a function of annealing time for films cast at 295 K and annealed at 407 K. The numbers beside each line indicate the P2VN guest bulk concentration in the PnBMA host. Filled points represent cloudy films and open points represent clear films. Standard deviations are less than 10% in this and subsequent plots of  $I_D/I_M$ .

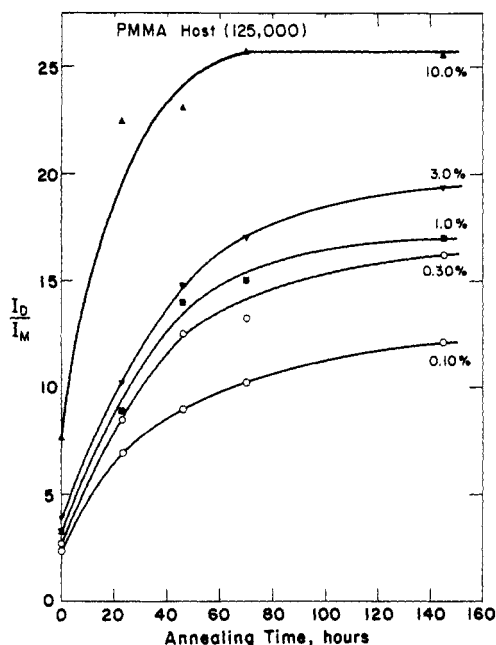


**Figure 2.** Observed  $I_D/I_M$  fluorescence ratio as a function of annealing time for films cast at 295 K and annealed at 407 K. The numbers beside each smooth line indicate the P2VN guest bulk concentration in PMMA host films. Filled points represent cloudy films and open points represent clear films.

peratures presented previously.<sup>4</sup> First, it was necessary to correct for interference from the slight background fluorescence. The observed  $I_D/I_M$  was corrected by subtracting the contribution to the excimer and monomer band intensities observed for a blank host film. Both fluorescence spectra of the pure host and the blend films were obtained under the same experimental conditions. This correction was significant only for the very low concentration blends (<0.5%) for which the excimer and monomer intensities are small. In the worst cases, the corrections amounted to 15% of  $I_M$  and 5% of  $I_D$  for the

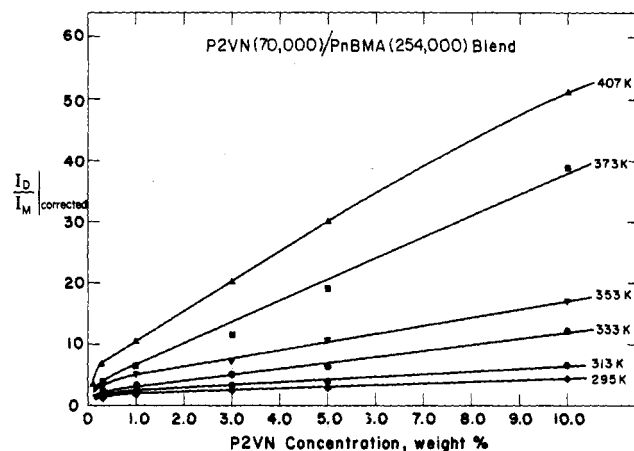


**Figure 3.**  $I_D/I_M$  corrected for spectral overlap of excimer and monomer as a function of P2VN guest bulk concentration for PnBMA host films cast at various temperatures and for films cast at 295 K and annealed at 407 K for 145 h.

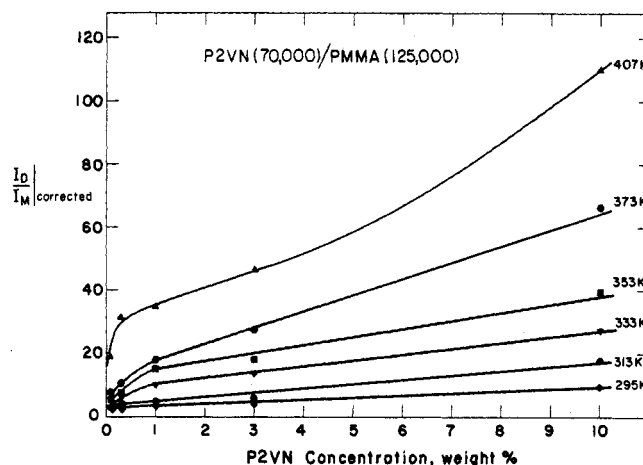


**Figure 4.**  $I_D/I_M$  corrected for spectral overlap of excimer and monomer as a function of P2VN guest bulk concentration for PMMA host films cast at various temperatures and for films cast at 295 K and annealed at 407 K for 145 h.

P2VN/PMMA blends and 30% of  $I_M$  and 10% of  $I_D$  for the P2VN/PnBMA blends.

Second, a correction procedure is needed to remove excimer/monomer band overlap and to give the true value of  $I_D/I_M$ . The experimental excimer band envelope intensity,  $I_D^e(398)$ , is assumed to be composed of the pure excimer intensity,  $I_D^o(398)$ , plus a fixed fraction,  $A$ , of the pure monomer band intensity,  $I_M^o(398)$ , measured at the excimer wavelength of 398 nm. Similarly, the experimental monomer envelope intensity  $I_M^e(331)$  consists of contributions from the pure monomer  $I_M^o(331)$  plus a fixed fraction,  $B$ , of the pure excimer band intensity,  $I_D^o(331)$ . This leads to

$$\frac{I_D^o(398)}{I_M^o(331)} = \frac{[I_D^e(398)/I_M^e(331)] - A}{1 - B [I_D^e(398)/I_M^e(331)]} \quad (1)$$

where  $A = B = 0.03$ .

$I_D/I_M$  data from the previous study<sup>4</sup> have been corrected and replotted in Figures 3 and 4. Figures 3 and 4 also include the corrected long-time results of the annealing experiments for P2VN/PnBMA and P2VN/PMMA blends, respectively.

## Discussion

**A. Two-Phase Photophysical Model.** Whenever the blend bulk composition exceeds the binodal composition

or the temperature is varied causing the blend composition to cross the binodal, phase separation can take place, resulting in a two-phase system. The degree of phase separation that takes place is expected to be dependent on both thermodynamic and kinetic effects. A photophysical model that can predict the equilibrium values of  $I_D/I_M$  for phase-separated blends has been proposed by Semerak<sup>14</sup> and Gelles<sup>10</sup> for the purpose of providing a comparison between the equilibrium and actual  $I_D/I_M$  values. This was initially applied to analyze thermally induced phase separation in initially miscible PS/PVME blends.<sup>10-12</sup> We present it here in a somewhat modified form that allows easier application to the highly incompatible P2VN/poly(alkyl methacrylate) blends.

There are two basic assumptions of the model: (i) the concentration of the P2VN fluorescent polymer is uniform within each phase and (ii) the fluorescence behavior of each phase is identical with that of a miscible blend whose bulk concentration equals the concentration within the phase. In effect, we are assuming that there is negligible energy transfer between the two phases.

The validity of these assumptions can be justified for the P2VN/PnBMA and P2VN/PMMA blends on two bases. First, earlier binodal calculations have indicated that the P2VN concentration in the lean phase is quite small.<sup>4</sup> Hence, P2VN coils should be isolated so that the probability of intermolecular electronic excitation transport is small. Second, an excitation in the P2VN-rich phase should not be able to make enough hops without being trapped to escape a concentrated phase that is large enough to scatter light.

In the absence of quenchers, the observed ratio of excimer to monomer fluorescence intensities corrected for any overlap of excimer and monomer bands is given by<sup>16</sup>

$$R_{\text{obsd}} \equiv \frac{I_D^0}{I_M^0} = \frac{Q_D}{Q_M} \left( \frac{1-M}{M} \right) \quad (2)$$

where  $Q_D/Q_M$  ( $\equiv K$ ) is the ratio of intrinsic quantum yields for excimer and monomer fluorescence and  $M$  is the overall probability that an absorbed photon leads to monomer emission by both radiative and nonradiative means. Provided that  $Q_D/Q_M$  does not depend on the phase, it is easy to show that the observed ratio for an  $m$ -phase system is given by

$$R_{\text{obsd}} = \frac{Q_D}{Q_M} \left( \frac{1 - \sum_{i=1}^m \phi_i M_i}{\sum_{i=1}^m \phi_i M_i} \right) \quad (3)$$

Here  $\phi_i$  is the fraction of chromophores in phase  $i$  and  $M_i$  is the probability that an absorbed photon leads to monomer decay from phase  $i$ .

For simplicity we assume that there are two phases, one rich in P2VN and one lean in P2VN, with negligible interphase. We then must compute  $\phi_i$  for the lean phase, the rich phase, and the bulk composition. Let  $C$  be the volume fraction of aromatic polymer P2VN and designate  $C_B$ ,  $C_L$ , and  $C_R$  as the initial blend composition before phase separation, the lean-phase composition, and the rich-phase composition, respectively. Also, let  $v_L$  and  $v_R$  denote the volume fractions of the lean and rich phase, respectively. A volume balance of the aromatic polymer results in the following relation:

$$C_B = C_L v_L + C_R v_R \quad (4)$$

By the lever rule the volume fraction of the rich phase is

$$v_R = \frac{C_B - C_L}{C_R - C_L} \quad (5)$$

The fraction of chromophores in the rich phase,  $\phi_R$ , is

$$\phi_R = \frac{C_R v_R}{C_B} = \frac{C_R(C_B - C_L)}{C_B(C_R - C_L)} \quad (6)$$

If  $M_L$  and  $M_R$  are defined to be the probabilities of eventual monomer decay from the lean and rich phases, then the observed fluorescence ratio for a two-phase system is given by

$$R_{\text{obsd}} = K \left[ \frac{\phi_R(R_R/K) + (1 - \phi_R)(R_L/K) + (R_L/K)(R_R/K)}{\phi_R(R_L/K) + (1 - \phi_R)(R_R/K) + 1} \right] \quad (7)$$

## B. Application of Two-Phase Photophysical Model.

The two-phase model involves five parameters:  $R_{\text{obsd}}$ ,  $R_R$ ,  $R_L$ ,  $\phi_R$ , and  $K$ . If the values of any four of these parameters are known, the remaining one can be readily calculated. In this section the model will be used first to calculate the  $I_D/I_M$  expected for each blend under the assumption that the separated phases represent the equilibrium binodal compositions. The calculated  $I_D/I_M$  will then be checked against the experimentally observed fluorescence ratio in order to assess the validity of the equilibrium assumption.

**1. P2VN/PnBMA Blends.** The equilibrium binodal compositions  $C_L$  and  $1 - C_R$  for this blend were evaluated earlier.<sup>4</sup> The P2VN-lean-phase composition,  $C_L$ , decreases from  $8.6 \times 10^{-2}$  at 295 K to  $1.8 \times 10^{-3}$  at 373 K, while the P2VN composition in the P2VN-rich phase,  $C_R$ , increases from 0.996 at 295 K to practically unity at 373 K. Only those blends with an initial bulk P2VN concentration greater than  $C_L$  are expected to phase separate at equilibrium. In Figure 3 the only blends that are *not* expected to be phase separated at equilibrium are the 0.10% (295–373 K), 0.30% (295–353 K), 1.0% (295–333 K), 3.0% (295–313 K), and 5.0% (295 K) blends, where the casting temperature range is shown in parentheses. In fact, all of these films were optically clear, and all others prepared at higher casting temperatures were cloudy.

Since  $C_R$  is practically equal to unity, excimer fluorescence in the rich phase should be intermolecular with three-dimensional energy transfer. Hence,  $R_R$  is set equal to 142, the fluorescence ratio  $I_D^0(398)/I_M^0(331)$  observed for a neat P2VN film, corrected for overlap. Due to the relatively low P2VN concentration in the lean phase, the P2VN chains are expected to be isolated from one another allowing only intramolecular excimer formation and quasi-one-dimensional energy migration. Under these conditions,  $R_L$  should be independent of  $C_L$ ; thus, its value is set equal to 1.1, the lowest ratio observed for the P2VN/PnBMA blend films. A similar value of 1.06 has been reported<sup>6</sup> for a truly miscible blend of P2VN in low molecular weight PS.

$Q_D/Q_M$  has been observed to depend on the temperature at which fluorescence is examined and on whether excimer formation is intermolecular or intramolecular.<sup>17-19</sup> Experimentally determined values of  $Q_D/Q_M$  at 295 K for P2VN in low-concentration P2VN/PCMA blends have an average value of 0.42.<sup>20</sup> In addition,  $Q_D/Q_M$  has a value of 0.42 for PS at 295 K in a PS/PVME blend.<sup>10</sup> A value of 0.42 will be used for  $K$  in this work.

The most sensitive parameter of the model is  $\phi_R$ , the volume fraction of P2VN in the rich phase; for large values of  $\phi_R$ , a small change in  $\phi_R$  results in a large change in the value of the calculated  $I_D/I_M$ . With  $R_R$ ,  $R_L$ , and  $K$  known,

**Table I**  
Results of the Two-Phase Model for Excimer Fluorescence in the P2VN/PnBMA Blend

$T_{\text{cast}}$ , K	$C_{\text{bulk}}$ , wt %	$(\phi_R)_{\text{eq}}$	$R_{\text{calcd}}$	$R_{\text{obsd}}$ (corrected)	$(\phi_R)_{\text{exp}}$	$(\phi_R)_{\text{exp}}/(\phi_R)_{\text{eq}}$
295	0.10	0.090	1.25	4.51	0.700	7.79
313	0.05	0.302	1.75	3.51	0.620	2.05
	0.10	0.669	4.08	6.74	0.790	1.18
333	0.03	0.575	3.11	5.23	0.740	1.29
	0.05	0.738	5.21	6.45	0.785	1.06
	0.10	0.876	10.96	12.23	0.890	1.02
353	0.03	0.834	8.28	7.21	0.810	0.971
	0.05	0.903	13.80	10.77	0.873	0.967
	0.10	0.954	26.58	17.05	0.923	0.968
373	0.01	0.806	7.08	6.59	0.790	0.980
	0.03	0.936	20.26	11.73	0.885	0.945
	0.05	0.969	31.53	19.20	0.934	0.970
	0.10	0.982	53.51	39.07	0.972	0.990
407	0.001	0.642	3.75	3.44	0.610	0.950
annealed	0.003	0.874	10.84	6.99	0.804	0.920
	0.01	0.963	31.40	10.49	0.872	0.906
	0.03	0.988	67.00	20.21	0.936	0.947
	0.05	0.993	85.95	29.98	0.960	0.967
	0.10	0.996	105.62	51.19	0.981	0.985

the photophysical model expressed by eq 7 may be used in two ways. First, if the morphology of the solvent-cast P2VN/PnBMA blend is truly representative of equilibrium at the bulk concentration and casting temperature, and if the Flory-Huggins thermodynamics is an adequate theoretical approach, then the equilibrium volume fraction of chromophores in the rich phase,  $(\phi_R)_{\text{eq}}$ , may be calculated from eq 6 by using the binodal concentrations evaluated earlier.<sup>4</sup> This value of  $\phi_R$  may then be substituted in eq 7 to obtain  $R_{\text{calcd}}$ . Alternatively, the observed value of  $R$ , corrected for scattering and excimer/monomer overlap, can be used with eq 7 to determine an experimental value of  $\phi_R$ .

Both approaches were taken to yield the results in Table I. For the annealed films and those cast at temperatures much higher than the blend  $T_g$ , the calculated fluorescence ratios are generally greater than the corresponding corrected experimental ones. As the casting temperature is lowered, both calculated and observed ratios become closer, and eventually the calculated ratios become smaller than the observed ones. A reasonable measure of the degree to which thermodynamic equilibrium has been reached in a blend is the ratio of the experimental value  $(\phi_R)_{\text{exp}}$  to the equilibrium value  $(\phi_R)_{\text{eq}}$ . These ratios indicate that for phase-separated blends cast at 353 and 373 K and films annealed at 407 K the separated phases have achieved over 94% of their equilibrium compositions. Although  $(\phi_R)_{\text{exp}}/(\phi_R)_{\text{eq}}$  seems to increase with P2VN bulk concentration, it is essentially constant at a given bulk concentration for the three highest temperatures.

For blends cast at 295, 313, and 333 K, however,  $(\phi_R)_{\text{exp}}/(\phi_R)_{\text{eq}}$  is greater than unity. This physically unreasonable result is a consequence of the fact that the observed  $I_D/I_M$  values for these blends are larger than predicted by the model. This, in turn, is caused by the fact that the observed  $I_D/I_M$  values actually increase with higher P2VN bulk concentration in the miscible region at the lowest P2VN compositions. For a truly miscible blend,  $I_D/I_M$  should be independent of P2VN bulk concentration unless the concentration is high enough or the chain extremely contracted to cause the energy-transfer process to change from one to three dimensional.

The minimum concentration at which the energy-transfer process becomes three dimensional has been estimated to be about 60% PS by volume for miscible blends of PS/PVME.<sup>10</sup> The calculation was based on the as-

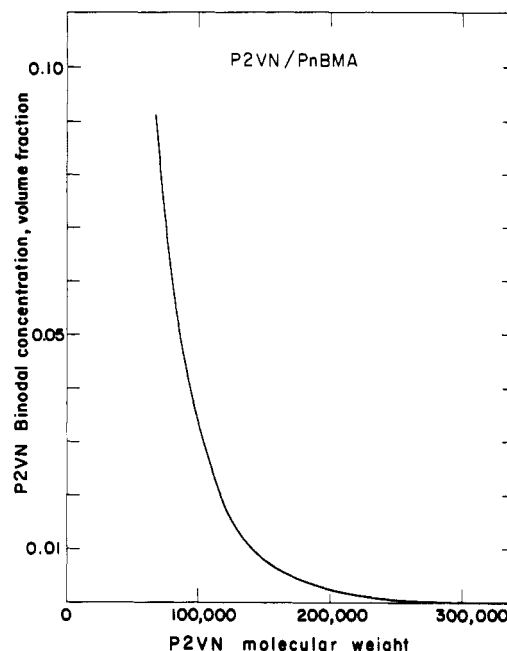


**Figure 5.** Dependence of the binodal composition of the P2VN-lean phase on the P2VN molecular weight at 295 K.

sumption that this minimum concentration corresponds to the point at which the average chromophore separation is equal to the Förster radius. Similar calculations performed for P2VN/PnBMA blends indicate that the minimum P2VN concentration for three-dimensional energy transfer should be 14% P2VN by volume.

In the miscible region for the blends studied in this work, the P2VN concentration is low enough ( $\leq 8.6\%$  at 295 K,  $\leq 3.3\%$  at 313 K, and  $\leq 1.26\%$  at 333 K) to suggest that energy migration should have an appreciable one-dimensional character. Hence, the observed  $I_D/I_M$  values would be expected to be constant up to the point of incipient phase separation as long as there is no change in the global conformational structure of the random coil. Since this is not the case, it is worthwhile to have a closer look into the procedure used to determine the miscible region for this blend for a possible cause of this discrepancy.

All the binodal calculations were made assuming monodisperse polymers, while the P2VN and PnBMA samples used to prepare the blends are, in fact, polydisperse. The P2VN binodal composition is very sensitive to P2VN molecular weight, however. This is shown in Figure 5 where the P2VN-lean-phase binodal concentration is plotted as a function of P2VN molecular weight at 295 K. Similar behavior is expected at higher temperatures. A P2VN sample with molecular weight larger than the viscosity-average molecular weight of 71 000 can result in a much narrower miscibility region than has been predicted. Hence, the polydispersity of the P2VN sample could initiate a fractionation process during which some of the higher molecular weight P2VN chains could phase separate at lower bulk concentrations earlier than expected.<sup>21</sup> This could lead to formation of microphases that are too small to scatter light but which, nevertheless, could act to increase the observed  $I_D/I_M$ . Unfortunately, this effect cannot be analyzed quantitatively due to the lack of molecular weight distribution data and the possible failure of the assumption of no energy transfer between the phases. However, fractionation is expected to be a significant problem only in those blends that are cast at low temperatures where solvent evaporation is slow.

To account for the fractionation process semiquantitatively, we have taken  $R_L$  to be equal to the actual ratio

**Table II**  
Modified Results of the Two-Phase Model for Excimer Fluorescence in the P2VN/PnBMA Blend

$T_{\text{cast}},$ K	$C_{\text{bulk}},$ wt %	$(\phi_R)_{\text{eq}}$	$R_{\text{calcd}}$	$R_{\text{obsd}}$ (corrected)	$(\phi_R)_{\text{exp}}$	$(\phi_R)_{\text{exp}}/$ $(\phi_R)_{\text{eq}}$
295	0.10	0.090	4.58	4.51	0.076	0.845
313	0.05	0.302	3.78	3.51	0.253	0.840
	0.10	0.669	8.16	6.74	0.600	0.897
333	0.03	0.575	5.28	5.23	0.570	0.980
	0.05	0.738	8.59	6.45	0.650	0.880
	0.10	0.876	17.36	12.23	0.820	0.940

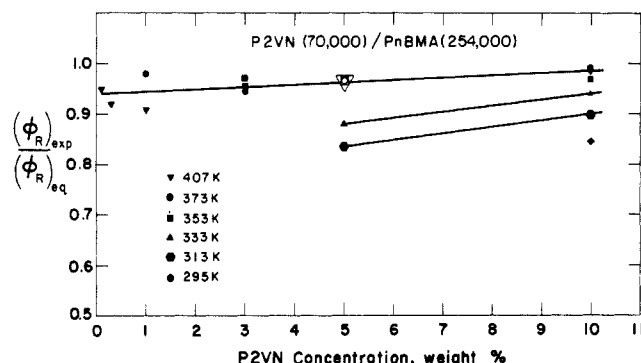


**Figure 6.** Dependence of the ratio of the actual fraction of chromophores in the P2VN-rich phase to its equilibrium value on bulk concentration of P2VN as a guest in PnBMA for films cast or annealed at elevated temperatures. The casting temperature is indicated beside each plotting symbol. The 407 K line represents results of the annealed films.

observed for a blend with the binodal composition. For example, the corrected fluorescence ratios from P2VN/PnBMA blends with binodal compositions of 8.6% P2VN at 295 K, 3.3% at 313 K and 1.26% at 333 K are 4.15, 2.50, and 2.10, respectively. The incorporation of these values in the application of eq 7 to blends cast at 295, 313, and 333 K yields results that are compatible with those of high casting temperatures. Table II shows these results; note that now the  $(\phi_R)_{\text{exp}}/(\phi_R)_{\text{eq}}$  ratios are less than unity. It is also observed that while  $(\phi_R)_{\text{exp}}/(\phi_R)_{\text{eq}}$  values increase, in general, with P2VN bulk concentration, they are lower than those at higher temperatures.

Results from Tables I and II are plotted in Figure 6. It is obvious that all the P2VN/PnBMA blends have achieved a high percentage (>84%) of their equilibrium composition and, as expected, the approach to equilibrium can be enhanced by either casting or annealing at higher temperatures.

In Figure 7,  $I_D/I_M$  is plotted as a function of  $(\phi_R)_{\text{eq}}$ . The solid line represents the two-phase model results for  $R_{\text{calcd}}$ , while the points are the experimentally observed data,  $R_{\text{obsd}}$  (corrected). The model fits the data points reasonably well. Hence, the assumption of attainment of equilibrium compositions for the two separated phases appears valid for the P2VN/PnBMA blend.

**2. P2VN/PMMA Blends.** The Flory-Huggins equilibrium binodal calculations for this blend were also presented earlier.<sup>4</sup> They indicate that over the temperature range of 295–373 K  $C_L$  is insignificantly low ( $<10^{-7}$ ) while  $C_R$  is practically unity if the separated phases have attained their equilibrium compositions. Thus, every one of the P2VN/PMMA blends is expected to be phase separated at equilibrium, and all of the films should be cloudy. However, this was not the case; the 0.1% (295–313 K) and 0.3% (295 K) blends were clear, while all others were cloudy. With these values of  $C_L$  and  $C_R$  and the P2VN bulk concentrations used in this study, it has been found from eq 6 that all values of  $\phi_R$  tend to approach unity

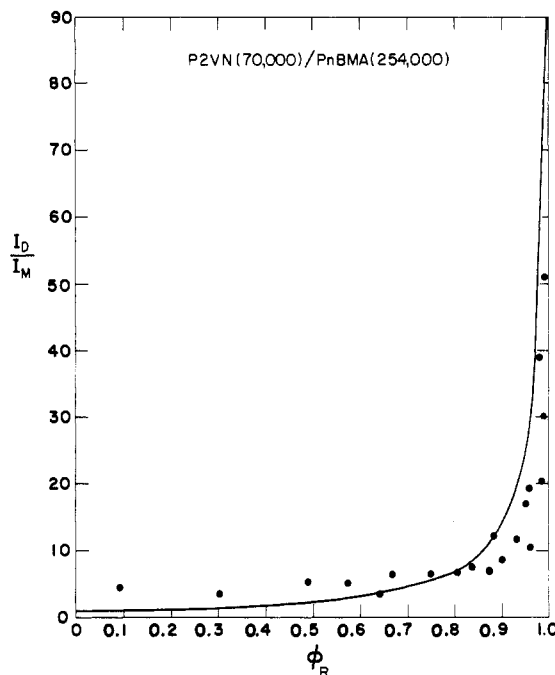


**Figure 7.** Comparison of experimental results for the dependence of the corrected ratio of excimer to monomer fluorescence intensities,  $I_D/I_M$ , for P2VN/PnBMA blends on the fraction of P2VN in the P2VN-rich phase,  $\phi_R$ , with the two-phase model predictions: (●) experimental data; the solid line shows the fit of the model.

**Table III**  
Results of the Two-Phase Model for Excimer Fluorescence in the P2VN/PMMA Blend

$T_{\text{cast}},$ K	$C_{\text{bulk}}$	$(\phi_R)_{\text{eq}}$	$R_{\text{calcd}}$	$R_{\text{obsd}}$ (corrected)	$(\phi_R)_{\text{exp}}$	$(\phi_R)_{\text{exp}}/$ $(\phi_R)_{\text{eq}}$
295	0.001	0.9993	133.3	2.55	0.493	0.493
	0.003			2.91	0.550	0.550
	0.01			3.63	0.631	0.631
	0.03			4.38	0.691	0.691
	0.10	1.00	142	9.81	0.860	0.860
313	0.001	0.9995	139.5	3.14	0.578	0.578
	0.003			4.0	0.663	0.663
	0.01			4.51	0.700	0.700
	0.03			5.71	0.760	0.760
	0.10	1.00	142	17.75	0.926	0.926
333	0.001	0.9997	141	4.26	0.682	0.682
	0.003			5.99	0.771	0.771
	0.01			10.14	0.865	0.865
	0.03			13.05	0.897	0.897
	0.10	1.00	142	27.22	0.955	0.955
353	0.001	1.0	142	5.57	0.755	0.755
	0.003	1.0	142	7.43	0.815	0.815
	0.01	1.0	142	15.28	0.913	0.913
	0.03	1.0	142	17.98	0.927	0.927
	0.10	1.0	142	39.54	0.972	0.972
373	0.001	1.0	142	7.43	0.815	0.815
	0.003	1.0	142	10.84	0.874	0.874
	0.01	1.0	142	17.51	0.926	0.926
	0.03	1.0	142	27.55	0.956	0.956
	0.10	1.0	142	66.38	0.987	0.987
407 annealed	0.001	1.0	142	18.95	0.932	0.932
	0.003	1.0	142	31.46	0.963	0.963
	0.01	1.0	142	34.64	0.967	0.967
	0.03	1.0	142	46.34	0.978	0.978
	0.10	1.0	142	110.22	0.997	0.997

(>0.999). Hence, the fluorescence ratio calculated by using eq 7 should approach that for a neat P2VN film. However, the experimentally observed values of the fluorescence ratio listed in Table III show that for the majority of the blends  $R_{\text{obsd}}$  is much smaller than  $R_{\text{neatP2VN}}$ .

The disagreement between the calculated and observed ratios is not unexpected for this blend. This is because

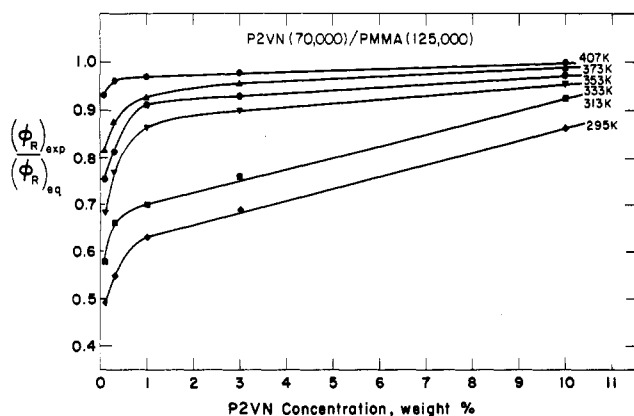


**Figure 8.** Dependence of the ratio of the actual fraction of chromophores in the P2VN-rich phase to its equilibrium value on bulk concentration of P2VN as a guest in PMMA for films cast or annealed at elevated temperatures. The casting temperature is indicated beside each line. The 407 K line represents results of the annealed films.

the phase-separated blends are in a nonequilibrium state due to the fact that all films have been cast at temperatures lower than the blend glass transition temperature. The incomplete phase separation that has taken place in the blends may result in either or both  $C_L$  and  $C_R$  being different from their equilibrium values. Since most of the blends are initially in the metastable region, phase separation is expected to take place via nucleation and growth. Hence,  $C_R$  should be equal to its equilibrium value of unity while  $C_L$  should be different from its equilibrium value.  $C_L$  is also expected to be dependent on both the bulk concentration and casting temperature. However, now that  $C_L$  is not equal to the equilibrium prediction, it is not clear how  $C_L$  should vary with  $C_{\text{bulk}}$  and  $T_{\text{cast}}$ .

The departure from equilibrium in the different blends may be estimated by using the two-phase model to calculate the actual value of the fraction of P2VN in the rich phase,  $(\phi_R)_{\text{exp}}$ , for each blend that makes  $R_{\text{obsd}} = R_{\text{calcd}}$ . The ratio of  $(\phi_R)_{\text{exp}}$  to its equilibrium value  $(\phi_R)_{\text{eq}}$  would then give a measure of how far from equilibrium the blend composition is. Values of  $(\phi_R)_{\text{exp}}$  and  $(\phi_R)_{\text{exp}}/(\phi_R)_{\text{eq}}$  are listed in Table III. Figure 8 also shows  $(\phi_R)_{\text{exp}}/(\phi_R)_{\text{eq}}$  plotted versus P2VN bulk concentration for the annealing and casting temperatures.  $(\phi_R)_{\text{exp}}/(\phi_R)_{\text{eq}}$  increases with concentration for a given  $T_{\text{cast}}$  and with casting temperature for a given concentration. The increase is sharp and nonlinear up to a bulk concentration of 1% followed by a slower and apparently linear increase in the region 1–10%.

### C. Annealing Kinetics for P2VN/PMMA Blends.

Although the primary thrust of this paper is to provide an explanation of the morphology resulting from solvent casting of marginally compatible polymer pairs, we are also interested in the time dependence of the annealing process. The annealing results for both P2VN/PnBMA and P2VN/PMMA were presented in Figures 1 and 2, and only the  $I_D/I_M$  values after long-term annealing ( $\sim 150$  h) have been analyzed to this point. In this section we wish to examine the kinetics of the P2VN/PMMA blends, for which sufficient data exist to obtain accurate time dependence.

The annealing experiment for the P2VN/PMMA films cast at 295 K was carried out at a temperature of 407 K, which is only 30 K above the  $T_g$  of PMMA and 2 K above the  $T_g$  of P2VN. In the absence of solvent, the molecular mobility should be very restricted and the driving force generated by the annealing temperature may not be enough to cause the small dispersed particles of the

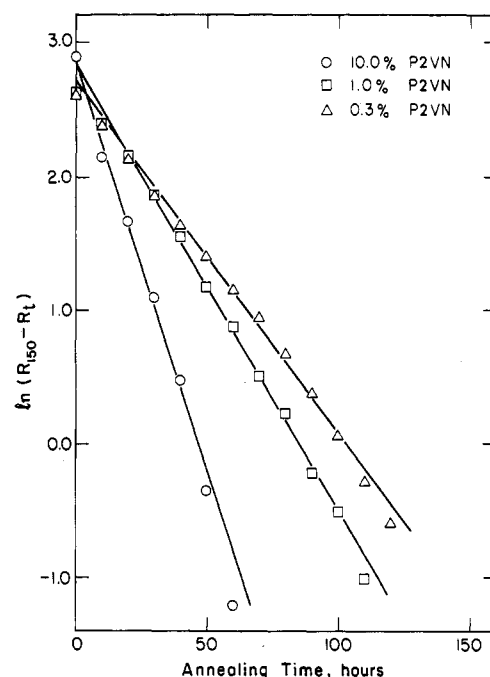


**Figure 9.** Analysis of the effect of annealing time at 407 K for P2VN/PMMA blends cast at 295 K.

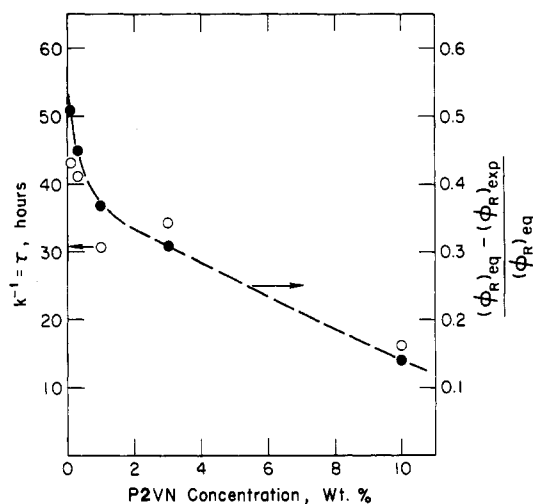


**Figure 10.** Left-hand scale: effect of P2VN concentration on the reciprocal of the annealing rate constant for P2VN/PMMA blends cast at 295 K and annealed at 407 K. Right hand scale: effect of P2VN concentration on the deviation from the equilibrium fraction of chromophores in the rich phase.

P2VN-rich domains to coalesce and grow in size to the extent that makes them scatter light and change from clear to cloudy. Nevertheless, the annealing procedure is expected to cause further microphase separation, which will increase the local P2VN-rich phase concentration and result in a large increase in the  $I_D/I_M$  values.

The general shape of the curves drawn through the annealing results of Figure 2 suggests that a fitting equation of the form

$$(R_{150} - R_t) = (R_{150} - R_0) \exp(-kt) \quad (8)$$

may be used. Here  $R \equiv I_D/I_M$ ,  $R_{150}$  is the value of  $I_D/I_M$  after 150 h of annealing at 407 K,  $R_t$  is the ratio after  $t$  h of annealing,  $R_0$  is the ratio of the 295 K cast blend prior to annealing, and  $k$  is the rate constant for the process. Representative plots for 10%, 1%, and 0.3% blends are shown in Figure 9. In general, this semilogarithmic form fits the data quite well for annealing times of 90 h or less. Deviations at longer times are probably due to slight errors

arising from an improper  $R_{150}$  value.

The rate constants derived from the plots of Figure 9 are shown in Figure 10 in the form of  $k^{-1} \equiv \tau$  as a function of P2VN concentration. Although the amount of data is somewhat limited, it is clear that the rate constant depends fairly strongly on P2VN concentration. Moreover, the effect is nonlinear with  $k$  increasing rapidly at very low concentrations and with  $k$  increasing more slowly at concentrations greater than 1%.

In an attempt to rationalize the concentration-dependent rate constant, we compared  $k^{-1}$  with a measure of the deviation from thermodynamic equilibrium. The quantity used was  $[(\phi_R)_{eq} - (\phi_R)_{exp}]/(\phi_R)_{eq}$ , where the  $(\phi_R)_{eq}$  and  $(\phi_R)_{exp}$  values have been taken from Table III. This parameter is plotted as the dashed line in Figure 10. There is extremely good agreement between the open data points and the dashed line, suggesting that the  $\tau$  value should be written

$$k^{-1} \equiv \tau = \tau_0 \left[ \frac{(\phi_R)_{eq} - (\phi_R)_{exp}}{(\phi_R)_{eq}} \right]$$

Thus, the closer the blend is to its equilibrium-phase morphology, the faster will be the change in local P2VN concentration toward the final equilibrium state.

**D. Ternary Phase Behavior.** The results of the elevated temperature casting experiments and the annealing experiments and the application of the two-phase model may be summarized as follows: First, some of the P2VN/PMMA blends are optically clear even though they are, in fact, thermodynamically immiscible. Second, some of the phase-separated P2VN/PnBMA blends are further away from equilibrium than expected for blends cast above  $T_g$ , while some of the phase-separated P2VN/PMMA blends have compositions much closer to equilibrium than expected for blends cast below  $T_g$ . Third,  $(\phi_R)_{exp}/(\phi_R)_{eq}$  increases with P2VN bulk concentration. Fourth,  $(\phi_R)_{exp}/(\phi_R)_{eq}$  increases with higher casting temperatures or by annealing above the blend  $T_g$ . While the last point may be explained by the greater molecular mobility provided by the lower blend viscosity at elevated temperatures, the first three cannot be explained satisfactorily based on the thermodynamics of binary polymer-polymer blends. It is possible, however, to resort to consideration of ternary phase diagrams to explain the results. Although the use of such phase diagrams in our discussion implies the existence of thermodynamic equilibrium, which is not the case for most of the PMMA host films, their use is very helpful as a reference point in understanding the results.

Equations 9–11 give Scott's<sup>22</sup> expressions for the volume fractions of solvent, polymer A, and polymer B at the plait point:

$$v_s = 1 - \frac{1}{2\chi_{AB}} \left( \frac{1}{x_A^{1/2}} + \frac{1}{x_B^{1/2}} \right)^2 \quad (9)$$

$$v_A = \frac{1}{2\chi_{AB}} \left( \frac{x_B^{1/2}}{x_A^{1/2} + x_B^{1/2}} \right) \left( \frac{1}{x_A^{1/2}} + \frac{1}{x_B^{1/2}} \right)^2 \quad (10)$$

$$v_B = \frac{1}{2\chi_{AB}} \left( \frac{x_A^{1/2}}{x_A^{1/2} + x_B^{1/2}} \right) \left( \frac{1}{x_A^{1/2}} + \frac{1}{x_B^{1/2}} \right)^2 \quad (11)$$

where  $\chi_{AB}$  is the binary interaction parameter of the two polymers and  $x$  is the degree of polymerization. Although these expressions are crude approximations, they nevertheless provide the essential features necessary to construct a schematic ternary phase diagram.

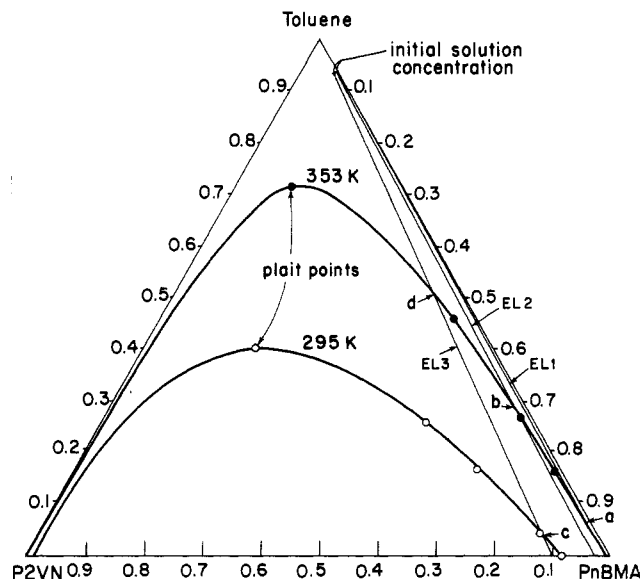


**Figure 11.** Schematic ternary phase diagrams for the P2VN/PnBMA/toluene system at temperatures of 295 and 353 K. All concentrations are weight fractions.

With the values of  $x_A$ ,  $x_B$ , and  $\chi_{AB}$  reported earlier for P2VN/PnBMA and P2VN/PMMA,<sup>4</sup> eq 9–11 were used to calculate the composition of the plait points for the P2VN/PnBMA/toluene and P2VN/PMMA/toluene systems at 295 and 353 K. The 295 K point has been chosen because it represents the lowest casting temperature. In addition, it is the casting temperature of the annealed blends. The 353 K point has been chosen because it represents the casting temperature at which all blends have been phase separated, as indicated by their cloudy appearance.

For the P2VN/PnBMA/toluene mixture, the plait point has a composition of 40.4% P2VN, 19.2% PnBMA, and 40.4% toluene by weight at 295 K. Corresponding values at 353 K are 19.4% P2VN, 9.1% PnBMA, and 71.5% toluene by weight. Three more points on the phase boundary were calculated corresponding to 30, 20, and 5 vol % toluene at 295 K and to 50, 30, and 20 vol % at 353 K. These three points, in addition to the plait point and the solvent-free binodal point, were used to construct the schematic phase diagrams at 295 and 353 K for the P2VN/PnBMA/toluene system shown in Figure 11.

The P2VN/PMMA/toluene mixture has plait point compositions of 8% P2VN, 6.5% PMMA, and 85.5% toluene by weight at 295 K and 6.1% P2VN, 6.5% PMMA, and 89% toluene by weight at 353 K. Three more points on the boundary line were calculated for 80, 70, and 50 vol % toluene. Figure 12 represents the schematic phase diagrams for the P2VN/PMMA/toluene ternary system at 295 and 353 K.

During casting, the film composition changes from that of the initial casting solution to the final composition, which may contain residual casting solvent. Each film with a different guest concentration passes along a distinct evaporation line. In Figure 11, three evaporation lines (EL1, EL2, and EL3) are drawn representing the casting process for the 0.3%, 3%, and 10% P2VN/PnBMA films. EL1 connects the initial solution composition point (92.9% toluene, 7.1% PnBMA,  $2.1 \times 10^{-2}\%$  P2VN by weight) and the point representing the final solvent-free composition of 99.7% PnBMA and 0.3% P2VN by weight. Note that EL1 does not cross the 295 K phase boundary, so a miscible one-phase system is obtained under these casting conditions. This is consistent with the observations that



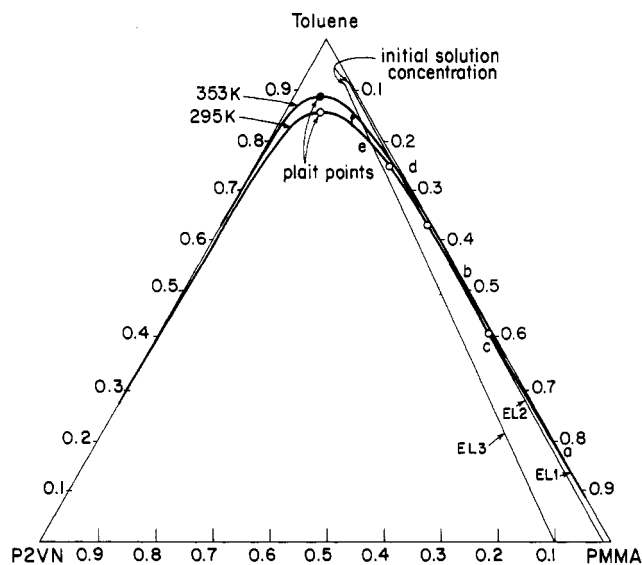


**Figure 12.** Schematic ternary phase diagrams for the P2VN/PMMA/toluene system at temperatures of 295 and 353 K. All concentrations are weight fractions.

films obtained for the 0.1% and 0.3% blends by solvent casting at 295 K are initially clear. This observation is reflected by the open plotting symbols at zero annealing time in Figure 1. EL1 does cross the 353 K boundary phase at point a, however, which should lead to phase separation. This is also consistent with the observation of translucent films for the 0.3% blends obtained by solvent casting at 353 K.

During the annealing experiment toluene is totally absent, leading to a high viscosity for the blend. It appears that, although the annealing temperature was high enough to create enough mobility to cause local phase separation and an increase in  $I_D/I_M$ , the P2VN concentration was too low to allow the growth of the P2VN dispersed particles to the size capable of scattering light. Hence, the 0.3% films remained clear even though the observed  $I_D/I_M$  ratio has increased as shown in Figure 1. A similar argument holds for the blends with the lowest guest concentration of 0.1%.

EL2 represents the evaporation path for blends with a guest concentration of 3%. Here again EL2 does not cross the 295 K phase boundary line, so it should lead to a clear one-phase film, as indicated by the open symbol in Figure 1. However, it does cross the 353 K phase boundary line at an intermediate state of evaporation (point b), leading to phase separation. The high temperature and presence of toluene at the point of phase separation allow the P2VN domains to grow in size yielding a cloudy film when solvent cast at 353 K, as reported earlier.<sup>4</sup> During the annealing process in the absence of solvent the higher bulk concentration of P2VN allows the P2VN domains to grow in size, resulting in a change in the film appearance from clear to cloudy. A similar argument applies to the 1.0 wt % blends.

Finally, EL3 represents the evaporation path for the 10 wt % films. Here EL3 crosses both the 295 and 353 K phase boundary lines, the former at a late stage of evaporation (point c) and the latter at an early stage (point d), resulting in both cases in large domain size for the phase-separated P2VN-rich regions and an initially cloudy appearance for the solvent-cast films. Figure 6 shows that, for the 10% films, the higher the casting temperature the larger is the fraction of P2VN in the P2VN-rich phase equilibrium composition that phase has attained, e.g.,  $(\phi_R)_{exp}/(\phi_R)_{eq} = 0.845$  at 295 K and 0.93 at 353 K. This is a direct result of the lower temperature and the smaller

amount of solvent present at point c compared to point d. The high annealing temperature compared to the blend  $T_g$  enhances further phase separation and growth for the P2VN-rich phase.

The P2VN/PMMA/toluene ternary phase diagram shown in Figure 12 shows appreciably different behavior compared to the P2VN/PnBMA/toluene system. It is obvious that the P2VN/PMMA polymer pair is much less thermodynamically compatible than the P2VN/PnBMA pair. This fact makes it more likely that there will be considerably more solvent and, thus, sufficient molecular mobility at the point where the evaporation lines cross the binodals, as compared to the P2VN/PnBMA/toluene systems. Without going through the details of an analogous treatment, we may conclude that, although there may be some kinetic restrictions to achieving phase equilibrium at P2VN concentrations of 0.1% and 0.3% cast at 295 K, all the higher concentration 295 K films and all of the films cast at 353 K should be very close to their equilibrium values, as was observed.

### Summary

The major conclusions are summarized below.

First, it has been shown that solvent casting at temperatures greater than  $T_g$  for the ternary polymer A/polymer B/solvent system, followed by rapid quenching to a temperature below  $T_g$ , can quench in the morphology characteristic of the casting temperature.

Second, use of the two-phase photophysical model has demonstrated that, although casting above  $T_g$  greatly enhances the chance of the two-phase separated blends attaining thermodynamic equilibrium, equilibrium is not guaranteed unless other kinetic barriers are also absent. Casting at temperatures much greater than  $T_g$  or annealing above the glass transition temperatures of both polymers further enhances the approach to equilibrium by reducing the kinetic effects.

Finally, the casting temperature and annealing experiments have demonstrated the ability of the modified Flory-Huggins theory with a temperature-dependent binary interaction parameter to predict the thermodynamics of solvent-cast polymer blends that are in equilibrium states.

**Acknowledgment.** Numerous helpful discussions with S. N. Semerak are gratefully acknowledged. This work was supported by the Polymers Program of the National Science Foundation under Grants DMR 79-16477 and DMR 84-07847.

**Registry No.** P2VN, 28406-56-6; PnBMA, 9003-63-8; PMMA, 9011-14-7.

### References and Notes

- (1) Frank, C. W.; Gashgari, M. A. *Macromolecules* **1979**, *12*, 163.
- (2) Frank, C. W.; Gashgari, M. A. *Ann. N.Y. Acad. Sci.* **1981**, *366*, 387.
- (3) Semerak, S. N.; Frank, C. W. *Macromolecules* **1981**, *14*, 443.
- (4) Gashgari, M. A.; Frank, C. W. *Macromolecules* **1981**, *14*, 1558.
- (5) Semerak, S. N.; Frank, C. W. *Adv. Chem. Ser.* **1983**, No. 203, 757.
- (6) Semerak, S. N.; Frank, C. W. *Macromolecules* **1984**, *17*, 1148.
- (7) Semerak, S. N.; Frank, C. W. *Adv. Chem. Ser.* **1984**, No. 206, 77.
- (8) Frank, C. W.; Gashgari, M. A.; Semerak, S. N. *NATO ASI Ser., Ser. C* **1986**, *182*, 523.
- (9) Gelles, R.; Frank, C. W. *Macromolecules* **1982**, *15*, 741.
- (10) Gelles, R.; Frank, C. W. *Macromolecules* **1982**, *15*, 747.
- (11) Gelles, R.; Frank, C. W. *Macromolecules* **1982**, *15*, 1486.
- (12) Gelles, R.; Frank, C. W. *Macromolecules* **1983**, *16*, 1448.
- (13) Frank, C. W.; Gelles, R. *NATO ASI Ser., Ser. C* **1986**, *182*, 561.
- (14) Semerak, S. N. Ph.D. Thesis, Stanford University, 1983.
- (15) We have reported separately<sup>3,6</sup> an  $I_D/I_M$  value for pure P2VN, uncorrected for spectral overlap, of 24, which utilized excimer and monomer wavelengths of 398 and 337 nm, respectively.



The difference in  $I_D/I_M$  arises from the choice of the monomer emission wavelength.

- (16) Fitzgibbon, P. D.; Frank, C. W. *Macromolecules* **1982**, *15*, 733.
- (17) Bokobza, L.; Jasse, B.; Monnerie, L. *Eur. Polym. J.* **1977**, *13*, 921.
- (18) Hirayama, F.; Lipsky, S. *J. Chem. Phys.* **1969**, *51*, 1939.

- (19) Cundall, R. B.; Robinson, D. A. *J. Chem. Soc., Faraday Trans. 2* **1972**, *68*, 1133.
- (20) Thomas, J. W., Jr.; Frank, C. W. *Macromolecules* **1985**, *18*, 1034.
- (21) Morawetz, H., personal communication.
- (22) Scott, R. L. *J. Chem. Phys.* **1949**, *17*, 279.

## Conformations of Diblock Copolymers in Dilute Solutions

Yushu Matsushita,\* Yasushi Nakao,<sup>1a</sup> Kunio Shimizu,<sup>1b</sup> Ichiro Noda, and Mitsuru Nagasawa<sup>1c</sup>

Department of Synthetic Chemistry, Nagoya University, Furo-cho, Chikusa-ku, Nagoya 464, Japan. Received November 17, 1987;  
Revised Manuscript Received February 8, 1988

**ABSTRACT:** Intrinsic viscosity measurements were carried out by using a series of diblock copolymers of polystyrene (PS) and poly(2-vinylpyridine) (P2-VP) with narrow molecular weight distributions in a common good solvent, pyridine, in a selective solvent, benzene, and in a poor solvent for both PS and P2VP, methyl ethyl ketone (MEK). Intrinsic viscosity-molecular weight relationships ( $[\eta]$ - $M$ ) for the two constituent homopolymers in pyridine are fortunately the same, and also, to our interest, that of the block copolymer is coincident with those of the homopolymers, while the exponents in the  $[\eta]$ - $M$  relationships as well as the magnitudes of  $[\eta]$  of the block copolymer in benzene and MEK are between those of the homopolymers. These facts imply that the block copolymer does not assume a distinct intramolecularly segregated conformation in dilute solutions, regardless of the nature of the solvents used.

### Introduction

Considerable efforts have been used to clarify whether or not chemically different blocks of diblock copolymers are segregated from each other in dilute solutions.<sup>2-16</sup> Although recent papers appear to succeed in revealing that an intramolecular segregation does not occur in dilute solutions,<sup>10,11,14</sup> the discussions for reaching the conclusion are not absolutely clear-cut because of large corrections for broad molecular weight distributions of constituting blocks in the block copolymer samples used.<sup>10</sup> It is also somewhat unsatisfactory for us that the molecular weight of the sample used for reaching the conclusion without any correction is very low if the phenomenon is an intramolecular phase separation.<sup>14</sup>

It is well established that the conformation of a homopolymer chain is determined by its unperturbed dimension and the excluded volume effects according to the two-parameter theory. Similar theoretical and Monte Carlo calculations<sup>8,17-20</sup> were applied to diblock copolymers, where the excluded volume effects are determined by the three excluded volume parameters between A-A, between B-B, and between A-B segments,  $\beta_{AA}$ ,  $\beta_{BB}$ , and  $\beta_{AB}$ , respectively. The former two parameters  $\beta_{AA}$  and  $\beta_{BB}$  are the same as those acting in the corresponding homopolymers. If we can use a diblock copolymer molecule consisting of two block chains, having the same unperturbed dimensions and excluded volume parameters, as a sample, the discussion of intramolecular segregation is very much simplified.

The diblock copolymers of polystyrene (PS) and poly(2-vinylpyridine) (P2-VP) were found to be suitable for the present purpose. The intrinsic viscosity-molecular weight relationships ( $[\eta]$ - $M$ ) of PS and P2-VP homopolymers are practically identical in pyridine, which is a common good solvent for both homopolymers, as well as in  $\theta$ -solvents. It is confirmed in a previous paper that anionically polymerized diblock copolymers of PS and P-2VP have very narrow molecular weight distributions with respect to the molecular weight of each block.<sup>21</sup> Moreover, PS and P2-VP

have considerably different solubility parameters,<sup>22</sup> and it was observed in phase separation experiments that they are incompatible even in pyridine, which is a common good solvent, unless the concentration is very low.<sup>23</sup>

### Experimental Section

**Materials.** The diblock copolymers of PS and P2-VP were prepared by an anionic polymerization method with a sequential monomer addition technique described in a previous work.<sup>21</sup> After complete consumption of styrene monomer, a portion of the polymerization solution was sealed off as a precursor for composition check.

Solvents used for measurements were benzene, *p*-dioxane, methyl ethyl ketone (MEK), pyridine, and tetrahydrofuran (THF). Benzene, which was of the spectroscopic grade by Merck, was used without further purification. The other solvents, which were of the special grade by Kishida Chemical Co., were dried according to standard procedures.

**Characterization.** The number-average molecular weights,  $M_n$ , were determined by osmometry in THF at 25 °C by using a Hewlett-Packard Type 502 high-speed membrane osmometer. The weight-average molecular weights,  $M_w$ , were determined by a light-scattering method in benzene, *p*-dioxane, and MEK at 25 °C by using a Fica 50 light-scattering photometer. The refractive index increments for PS and P2-VP are 0.109<sub>0</sub> and 0.106<sub>5</sub> in benzene, 0.185<sub>2</sub> and 0.176<sub>0</sub> in *p*-dioxane, and 0.229<sub>0</sub> and 0.214<sub>5</sub> in MEK, respectively. The polydispersity index  $M_w/M_n$  was calculated from the GPC chromatograms in THF, assuming that the calibration curve determined with pressure chemical standard polystyrenes is applicable to the block copolymers. Since THF is a common good solvent for both PS and P2-VP, we may safely assume that the values of  $M_w/M_n$  thus determined are close to the true values.

**Intrinsic Viscosity Measurements.** Viscosity measurements were carried out by using dilution viscometers of a modified Ubbelohde type in three solvents, pyridine, benzene, and MEK. Pyridine is a common good solvent for both PS and P2-VP, benzene is a selective solvent (i.e., a good solvent for PS but a poor ( $\theta$ ) solvent for P2-VP), and MEK is a poor solvent for both polymers. The  $\theta$ -temperature for P2-VP in benzene was previously found to be ca. 11 °C.<sup>24</sup> Measurements were carried out at 25.0 °C in pyridine and MEK and at 10.0 °C in benzene. Intrinsic viscosities of PS and P2-VP homopolymers were also measured